Supplement of Atmos. Chem. Phys., 18, 13969–13985, 2018
https://doi.org/10.5194/acp-18-13969-2018-supplement

Atmospheric Chemistry and Physics
Open Access
EGU

Supplement of

Daytime HONO, NO_2 and aerosol distributions from MAX-DOAS observations in Melbourne

Robert G. Ryan et al.

Correspondence to: Robert G. Ryan (rgryan@student.unimelb.edu.au)

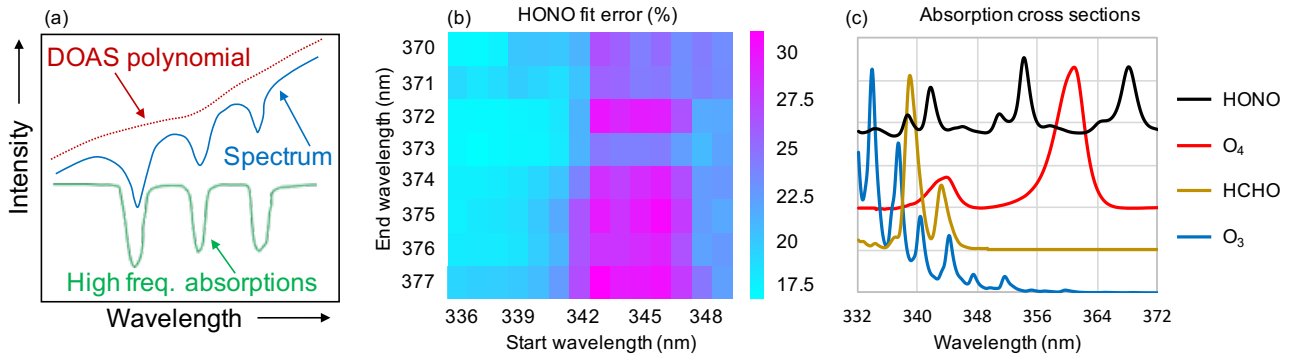

Figure S1. (a) Schematic of the DOAS principle, (b), HONO sensitivity study results using the retrieval interval mapping technique and (c) HONO, O_4, HCHO and O_3 cross sections plotted between 332 and 372 nm, showing the cross section overlap in the HONO fitting interval.

Table S1. Details of the DOAS settings in this work

Species	Cross section
O_3 (223 and 243 K)	Serdyuchenko et al. (2014)
NO_2 (220 and 298 K)	Vandaele et al. (1998)
O_4 (293 K)	Thalman and Volkamer (2013)
HCHO (297 K)	Meller and Moortgat (2000)
BrO (223 K)	Fleischmann et al. (2004)
HONO	Stutz et al. (2000)
Ring effect (293 K and 250 K)	Grainger and Ring (1962)
DOAS polynomial	5th order
Offset term	1st order

S1 Aerosol and trace gas retrieval tests

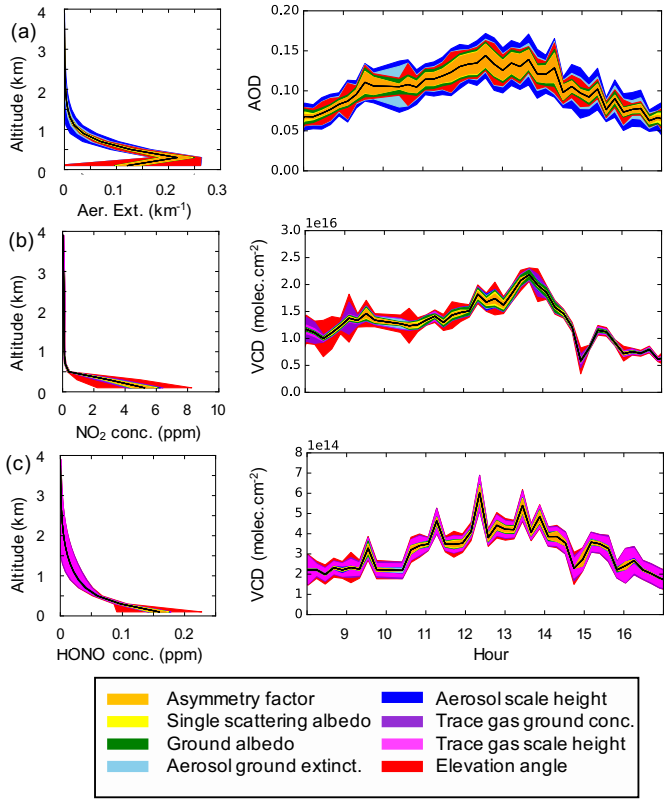

Figure S2. Results of a priori/forward model parameter tests for (a) an example aerosol extinction vertical profile (1 pm local time on 7th March 2017), left, and total aerosol optical depth (AOD) over the course of the day on 7th March 2017, right; (b) an example vertical concentration profile of NO_2 and NO_2 vertical column density (VCD); (c) same as (b) but for HONO. Each colour represents the mean $\pm$ the standard deviation attributable to the particular test parameter as indicated by the legend. Note that VCD values for NO_2 are to the power of 16, and HONO VCD values are to the power of 14.

Figure S2(a) shows the results from different parameter tests on aerosol optical depth (AOD) and an example aerosol extinction profile from the 7th of March. Each shaded region represents the mean $\pm$ the standard deviation attributable to each test. The vertical profile reveals a dominant contribution of a priori shape parameters (scale height and ground extinction, blue colours) to upper level uncertainty, with a 60% error contribution above 500 m. This is expected since the inherent higher sensitivity of the retrievals to the measurements at low altitudes, means the a priori profile more strongly constrains the retrieval at high altitudes. Below 500m, the influence of the shape parameters is much less significant at 10%, while the optical properties (yellow and green colours) play a more significant role with a 12% error. The balance of these contributions suggests that a priori shape parameters are a more significant error source than the forward model parameters, as observed in the plot of AOD

over the course of 7th March, highlighting that the inherent low sensitivity of MAX-DOAS retrievals to upper levels could be greatly improved with better knowledge of the a priori shape parameters. The influence of a $\pm 0.5^{\circ}$ elevation angle uncertainty, in red, is also included. These results indicate that a $\pm 0.5^{\circ}$ elevation angle uncertainty leads to a 35 $\%$ error in retrieved aerosol extinction close to the ground, and an 11 $\%$ error aloft, demonstrating the critical importance of a well calibrated elevation angle to successful MAX-DOAS retrievals.

Figures S2(b) and (c) show the results of the parameter tests on the NO_2 and HONO retrievals. At ground level the elevation angle term dominates the graph, highlighting the importance of elevation angle calibrations for reducing error in retrieved trace gas ground concentrations. The influence of the carry-over aerosol error and trace gas shape a priori parameters is shown to be small, between 3 and 4 $\%$ for in each case for both trace gases.

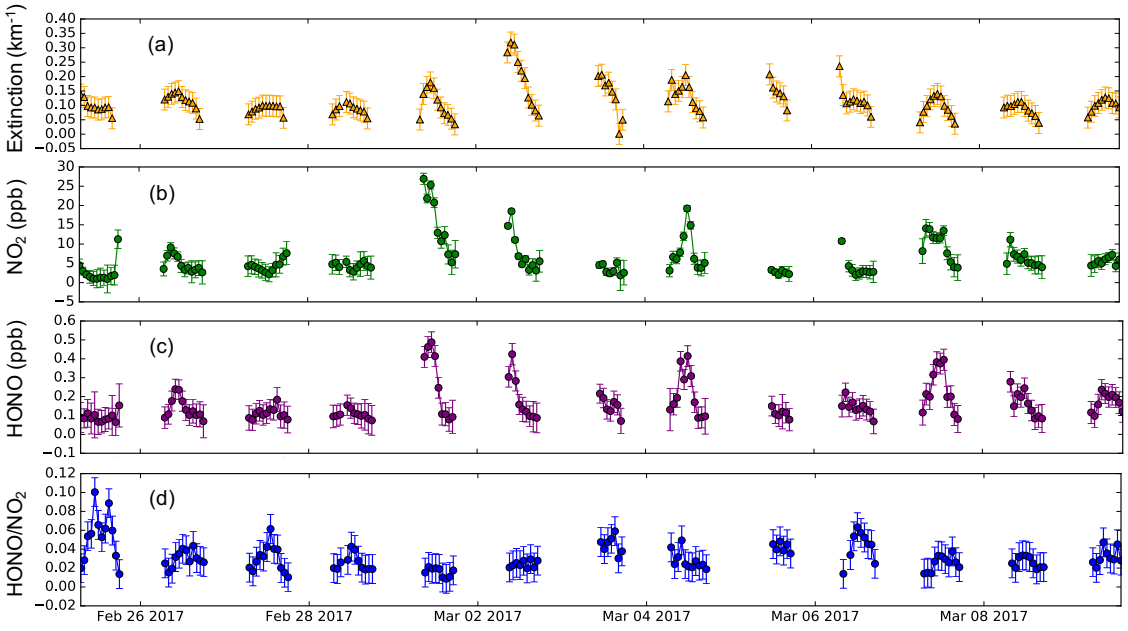

Figure S3. Example timeseries from 25/02/2017 to 10/03/2017 for aerosol optical depth, NO_2 surface concentration, HONO surface concentration and the ratio of HONO/NO_2 surface concentrations

Table S2. Compilation of urban HONO surface measurements from cities around the world. Average (avg) and maximum (max.) values are from diurnal cycles reported in the papers referenced, and therefore comparable with the diurnal cycle results in this work. It should be noted that the maximum HONO values reported from each paper listed occurred around or shortly after sunrise, as opposed to midday as in this work.

Reference	Location	Season, year	HONO meas. technique	Midday avg HONO (ppbv)	Max. HONO (ppbv)	Midday avg NO_2 (ppv)
Lee et al. (2016)	London, UK	Summer 2012	LOPAP	0.4	0.6	15*
Michoud et al. (2014)	Paris, France	Summer 2009	Wet chemical	0.1	0.2	3
Acker and Möller (2007)	Rome, Italy	Spring 2001	Wet chemical	0.2	0.9	7
Hendrick et al. (2014)	Beijing, China	Summer 2008	MAX-DOAS	0.2	1.0	23
Huang et al. (2017)	Xi'an, China	Summer 2015	LOPAP	0.4	2.2	11
Wang et al. (2013)	Shanghai, China	Summer 2011-12	LP-DOAS	0.6	1.2	15
Xu et al. (2015)	Hong Kong	Summer 2011	LOPAP	0.8	1.0	23
Ren et al. (2003)	New York City, USA	Summer 2001	HPLC	0.4	1.0	25*
Pusede et al. (2015)	Pasadena, USA	Summer 2010	CIMS	0.3	1.1	15
Wong et al. (2012)	Houston, USA	Spring 2009	LP-DOAS	0.1	0.3	7
Elshorbany et al. (2009)	Santiago, Chile	Autumn 2005	LOPAP	1.7	3.7	30
This work	Melbourne, Australia	Autumn 2017	MAX-DOAS	0.2	0.2	9

* NO_x reported rather than NO_2. LOPAP = long path absorption photometer, LP-DOAS = long path differential optical absorption spectrscopy, HPLC = high performance liquid chromatography, CIMS = chemical ionization mass spectrometery

Table S3. Compiled regression analysis for the temporal correlation between HONO and NO_2 volume mixing ratios in different retrieval layers.

Retrieval layers	Altitudes	Pearson's R coefficient	Regression slope
1	0-200 m	0.810	0.01
1 and 2	0-400 m	0.626	0.01
3 and 4	400-800 m	0.371	0.01
5 and 6	800-1200 m	0.260	0.004

References

Acker, K. and Möller, D.: Atmospheric variation of nitrous acid at different sites in Europe, Environmental Chemistry, 4, 242–255 1449–8979, 2007.

Elshorbany, Y., Kurtenbach, R., Wiesen, P., Lissi, E., Rubio, M., Villena, G., Gramsch, E., Rickard, A., Pilling, M., and Kleffmann, J.: Oxidation capacity of the city air of Santiago, Chile, Atmospheric Chemistry and Physics, 9, 2257–2273

Fleischmann, O. C., Hartmann, M., Burrows, J. P., and Orphal, J.: New ultraviolet absorption cross-sections of BrO at atmospheric temperatures measured by time-windowing Fourier transform spectroscopy, Journal of Photochemistry and Photobiology A: Chemistry, 168, 117–132 2004.

Grainger, J. F. and Ring, J.: Anomalous Fraunhofer Line Profiles, Nature, 193, 762–762, 1962.

Hendrick, F., Müller, J.-F., Clémer, K., Wang, P., Mazière, M. D., Fayt, C., Gielen, C., Hermans, C., Ma, J., and Pinardi, G.: Four years of ground-based MAX-DOAS observations of HONO and NO 2 in the Beijing area, Atmospheric Chemistry and Physics, 14, 765–781

Huang, R.-J., Yang, L., Cao, J., Wang, Q., Tie, X., Ho, K.-F., Shen, Z., Zhang, R., Li, G., and Zhu, C.: Concentration and sources of atmospheric nitrous acid (HONO) at an urban site in Western China, Science of The Total Environment, 593, 165–172, 2017.

Lee, J., Whalley, L., Heard, D., Stone, D., Dunmore, R., Hamilton, J., Young, D., Allan, J., Laufs, S., and Kleffmann, J.: Detailed budget analysis of HONO in central London reveals a missing daytime source, Atmospheric Chemistry and Physics, 16, 2747–2764, 2016.

Meller, R. and Moortgat, G. K.: Temperature dependence of the absorption cross sections of formaldehyde between 223 and 323 K in the wavelength range 225–375 nm, Journal of Geophysical Research: Atmospheres, 105, 7089–7101 2156–2202, 2000.

Michoud, V., Colomb, A., Borbon, A., Miet, K., Beekmann, M., Camredon, M., Aumont, B., Perrier, S., Zapf, P., and Siour, G.: Study of the unknown HONO daytime source at a European suburban site during the MEGAPOLI summer and winter field campaigns, Atmospheric Chemistry and Physics, 14, 2805–2822 1680–7316, 2014.

Pusede, S. E., VandenBoer, T. C., Murphy, J. G., Markovic, M. Z., Young, C. J., Veres, P. R., Roberts, J. M., Washenfelder, R. A., Brown, S. S., and Ren, X.: An atmospheric constraint on the NO2 dependence of daytime near-surface nitrous acid (HONO), Environmental Science & Technology, 49, 12 774–12 781, 2015.

Ren, X., Harder, H., Martinez, M., Lesher, R. L., Oliger, A., Simpas, J. B., Brune, W. H., Schwab, J. J., Demerjian, K. L., and He, Y.: OH and HO2 chemistry in the urban atmosphere of New York City, Atmospheric Environment, 37, 3639–3651

Serdyuchenko, A., Gorshelev, V., Weber, M., Chehade, W., and Burrows, J.: High spectral resolution ozone absorption cross-sections, Atmospheric Measurement Techniques, 7, 1867–8548, 2014.

Stutz, J., Kim, E., Platt, U., Bruno, P., Perrino, C., and Febo, A.: UV visible absorption cross sections of nitrous acid, Journal of Geophysical Research: Atmospheres, 105, 14 585–14 592, 2000.

Thalman, R. and Volkamer, R.: Temperature dependent absorption cross-sections of O 2–O 2 collision pairs between 340 and 630 nm and at atmospherically relevant pressure, Physical chemistry chemical physics, 15, 15 371–15 381, 2013.

Vandaele, A. C., Hermans, C., Simon, P. C., Carleer, M., Colin, R., Fally, S., Merienne, M.-F., Jenouvrier, A., and Coquart, B.: Measurements of the NO2 absorption cross-section from 42 000 cm-1 to 10 000 cm-1 (238–1000 nm) at 220 K and 294 K, Journal of Quantitative Spectroscopy and Radiative Transfer, 59, 171–184, 1998.

Wang, S., Zhou, R., Zhao, H., Wang, Z., Chen, L., and Zhou, B.: Long-term observation of atmospheric nitrous acid (HONO) and its implication to local NO2 levels in Shanghai, China, Atmospheric environment, 77, 718–724 1352–2310, 2013.

Wong, K., Tsai, C., Lefer, B., Haman, C., Grossberg, N., Brune, W., Ren, X., Luke, W., and Stutz, J.: Daytime HONO vertical gradients during SHARP 2009 in Houston, TX, Atmospheric Chemistry and Physics, 12, 635–652, 2012.

Xu, Z., Wang, T., Wu, J., Xue, L., Chan, J., Zha, Q., Zhou, S., Louie, P. K., and Luk, C. W.: Nitrous acid (HONO) in a polluted subtropical atmosphere: Seasonal variability, direct vehicle emissions and heterogeneous production at ground surface, Atmospheric environment, 106, 100–109 2015.